

## ORBITAL AND STELLAR PARAMETERS OF OMICRON LEONIS FROM SPECTROSCOPY AND INTERFEROMETRY

C. A. HUMMEL,<sup>1</sup> J.-M. CARQUILLAT,<sup>2</sup> N. GINESTET,<sup>2</sup> R. F. GRIFFIN,<sup>3</sup> A. F. BODEN,<sup>4</sup> A. R. HAJIAN,<sup>1</sup>  
D. MOZURKEWICH,<sup>5</sup> AND T. E. NORDGREN<sup>6</sup>

Received 2000 July 11; accepted 2000 November 29

### ABSTRACT

We present a three-dimensional solution for the orbit of the double star Omicron Leonis, based on new photoelectric radial velocity data mainly from the Observatoire de Haute-Provence and on interferometric data obtained with the Navy Prototype Optical Interferometer, the Mark III Stellar Interferometer, and the Palomar Testbed Interferometer. Omicron Leo's primary is a giant of type F9 and the secondary is an A5m dwarf, for which we derive masses of  $2.12 \pm 0.01 M_{\odot}$  and  $1.87 \pm 0.01 M_{\odot}$ , respectively. The distance to the binary is determined to be  $41.4 \pm 0.1$  pc. Combining the distance with the measured apparent magnitudes and color differences between the components yields luminosities of  $39.4 \pm 2.4 L_{\odot}$  and  $15.4 \pm 1.0 L_{\odot}$  for primary and secondary, respectively. Data from the Palomar Testbed Interferometer taken at  $2.2 \mu\text{m}$  are used to constrain the photometry in the infrared.

*Key words:* binaries: spectroscopic — binaries: visual — stars: fundamental parameters — stars: individual (*o* Leonis) — techniques: interferometric

### 1. INTRODUCTION

In the pursuit of ever more accurate mass determinations of stars in binary systems, two ground-based methods that have shown exceptional improvements in the precision of their measurements have joined forces. For favorable stellar systems, spectroscopy has reduced radial velocity measurement uncertainties to the meter-per-second level, whereas long-baseline optical interferometry has reduced the astrometric uncertainty of relative position measurements for the purpose of orbit determination to less than  $100 \mu\text{s}$ . Combined, they enable the determination of stellar masses with a relative uncertainty smaller than a few percent. This level of accuracy is needed to constrain current stellar evolution models.

We discuss in this paper *o* Leo, a double-lined spectroscopic binary, which is a good candidate for higher precision mass determinations for the following reasons. It consists of an F9 giant and an A5m dwarf, whose metallic lines are strong enough to be measured easily. The two components are not too different in brightness, which helps both the spectral analysis and the detection of the secondary by interferometry at separations of only a few milliarcseconds from the primary. The fairly high orbital inclination,  $i$ , makes the derived masses less sensitive to errors in the inclination than would be the case if  $i$  were low,

because the relative error in the mass is proportional to  $3/\tan i$  times the error in  $i$ .

Also known as HR 3852, FK5 365, HD 83808/9, and HIC 47508, *o* Leo is a 3.5 mag star about  $6^{\circ}$  south preceding Regulus. Several determinations of its *UBV* magnitudes (references given in Mermilliod & Mermilliod 1994) have given  $V = 3.52$  mag,  $(B - V) = 0.49$  mag,  $(U - B) = 0.21$  mag. Its brightness ensured that it was observed early in the era of photographic spectroscopy that dawned at the end of the nineteenth century, and it features in the very first list of composite-spectrum binaries, published by that most perceptive classifier Maury (1897). Maury found it to consist of a component similar to Procyon with a companion a little later than Sirius. We cannot do much better than that today, apart from recognizing that the star of later type must be a more evolved star than Procyon, since its luminosity is greater than that of the earlier one; the comparison with Sirius was inspired, since that star, like *o* Leo, is a metallic-lined one. Omicron Leo's spectroscopic duplicity led to its being listed in the Henry Draper Catalogue (Cannon & Pickering 1919) with two numbers, HD 83808 (type F5) and 83809 (A3).

Hardly had its composite nature been recognized than radial velocity observations of *o* Leo started at the Lick Observatory, with the original Mills Spectrograph (Campbell 1898a) on the 36 inch (0.9 m) refractor. Large velocity variations were immediately apparent and were announced by Campbell (1898b); early in the following year he (Campbell 1899) further announced the period to be 14.5 days—a value differing by little more than 0.01% from the one that we establish in the present paper. A double-lined orbit was published by Zurhellen (1907) on the basis of 12 spectrograms taken with the 12 inch (0.3 m) Repsold refractor at Bonn; in the following year, very similar elements were derived from 41 Lick observations by Plummer (1908), whose paper includes the interesting aside, “The inclination of the orbit must remain unknown . . .”

Plummer's orbit is still current; it appears (No. 580) in the Eighth Catalogue of the Orbital Elements of Spectroscopic Binary Systems (Batten, Fletcher, & MacCarthy 1989), with

<sup>1</sup> Astrometry Department, US Naval Observatory, 3450 Massachusetts Avenue NW, Washington, DC 20392; cah@gemini.usno.navy.mil, hajian@gemini.usno.navy.mil.

<sup>2</sup> Observatoire Midi-Pyrénées, Laboratoire d'Astrophysique, 14 Avenue Edouard Belin, F-31400 Toulouse, France; carquila@obs-mip.fr, ginestet@obs-mip.fr.

<sup>3</sup> The Observatories, Cambridge University, Madingley Road, Cambridge CB3 0HA, England, UK; rfg@ast.cam.ac.uk.

<sup>4</sup> Jet Propulsion Laboratory, California Institute of Technology, 4800 Oak Grove Drive, Pasadena, CA 91109; member of the PTI Collaboration; bode@huey.jpl.nasa.gov.

<sup>5</sup> Remote Sensing Division, Naval Research Laboratory, 4555 Overlook Avenue SW, Washington, DC 20375; dm@gemini.usno.navy.mil.

<sup>6</sup> US Naval Observatory, NPOI, P.O. Box 1149, Flagstaff, AZ 86002; nordgren@sextans.lowell.edu.

the note that relatively recent measures by Parsons (1983) confirm it. Parsons's material consisted of seven Reticon spectra taken at the McDonald 2.1 m reflector; they seem to have yielded velocities for the primary star only (perhaps because at their wavelength of  $\sim 6120 \text{ \AA}$  the A-type star appears relatively weaker than it does in the violet), but in three of the seven cases the velocity is so near to the systemic velocity  $\gamma$  that it must be affected by blending. The McDonald velocities, while consonant with Plummer's orbit, showed that the phase had slipped slightly from the ephemeris and warranted the introduction of a fifth decimal place in the period. The only other published radial velocities of which we are aware are three obtained at the Cape of Good Hope (Lunt 1919; Jones 1928); two of them are blends, the third being of the primary only.

Radial velocities attributed to  $\sigma$  Leo by Frost, Barrett, & Struve (1929) are not of  $\sigma$  Leo at all but are of 95 Leo. The same mistake occurs in other papers, including the one by Struve & Morgan (1927) that presents an orbit for 95 Leo. It arises through confusion between Greek omicron and "oh," as (for safety) we call the ordinary lowercase roman letter here: 95 Leo is also oh Leo. The distinction is difficult, sometimes impossible, to see in print, but in the papers cited above 95 Leo is definitely identified as omicron Leo. The error was carried over into the Sixth Catalogue of the Orbital Elements of Spectroscopic Binary Systems (Batten 1967) but has been corrected in subsequent editions. It can be traced all the way back to Baily (1845), whose work is often taken as the ultimate arbiter of constellation designations. Another instance of the same confusion was noted very recently (Griffin 1999) in a different context.

Several efforts, all of them unsuccessful because of the smallness of the angular separation, have been made in the past to resolve  $\sigma$  Leo directly. Merrill (1922) tried to do so with the interferometer of Anderson (1920) on the Mount Wilson 100 inch (2.5 m) reflector. Speckle interferometry has been equally unavailing (McAlister et al. 1993). The star is near enough ( $\sim 3''.5$ ) to the ecliptic to be occulted by the Moon, as was pointed out by Schmidtke (1979); it appears in the Zodiacal Catalog (Robertson 1940) as No. 1428. An occultation was actually observed by Africano et al. (1978), but the system was not resolved.

In the present investigation, observations of  $\sigma$  Leo were obtained by photoelectric radial velocity spectrometers, mainly the CORAVEL instrument at the Observatoire de Haute-Provence (OHP; Baranne, Mayor, & Poncet 1979), the Mark III Stellar Interferometer (Mark III; Shao et al. 1988), the Navy Prototype Optical Interferometer (NPOI; Armstrong et al. 1998), and the Palomar Testbed Interferometer (PTI; Colavita et al. 1999). The data from those instruments were combined to allow the derivation of orbital elements and physical parameters, including the mass and luminosity of the components.

## 2. SPECTRAL CLASSIFICATION

The component classifications of  $\sigma$  Leo are given in the Bright Star Catalogue (Hoffleit & Jaschek 1982) as F6 II (proposed by Bidelman 1951) and A5 V (proposed by Bahng 1958) for primary and secondary, respectively. No one author had given both those types. These classifications are in need of revision, as the following evidence shows.

Since both components give correlation dips with CORAVEL (see Fig. 1), we know immediately that the

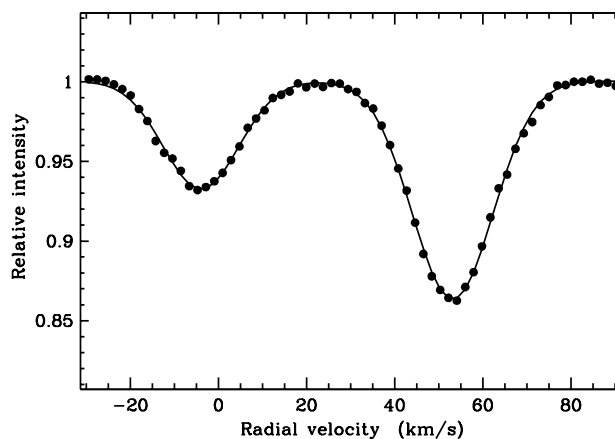


FIG. 1.—Double-lined example of a CORAVEL radial velocity trace, obtained at OHP on 1993 February 19.

hotter star must be chemically peculiar. From the  $v \sin i$  values of  $11.03 \pm 0.14 \text{ km s}^{-1}$  and  $8.12 \pm 0.27 \text{ km s}^{-1}$  for primary and secondary, respectively, we see that the low value for the hot secondary is consistent with it being an Am star, for which slow rotation is an expected characteristic.

An investigation in the blue to near-UV spectral region (Aurélié spectrograph, 380–420 nm,  $1.6 \text{ nm mm}^{-1}$ ) confirms the Am nature of the hot component. The metallic lines are as intense as in an F star, and the Sr II 4078 line is particularly strong, which can explain the erroneous classifications such as F6 II, in contradiction with both our observations in the near-infrared (see below) and the absolute combined visual magnitude of the system,  $M_V = +0.43$ . Furthermore, the 4173 (Fe II + Ti II) and 4179 (Fe II + Y II) blends exhibit intensities and profiles similar to those of Am stars and not like those of normal A5 V stars. All the observed characteristics are those of a metallic-lined star.

We applied to  $\sigma$  Leo the method of disentangling composite spectra by subtraction (Griffin & Griffin 1986), by using for the primary the spectrum of the MK standard 31 Com (G0 III, see below). The resulting spectrum is like the one of HD 179143/4, a known Am star (Babcock 1958; Markowitz 1969) also observed by us with the Aurélié spectrograph and classified by Markowitz as A5, F0, and F9 for the K line, the hydrogen lines, and the metallic lines, respectively. Markowitz also notes that "the spectrum (of HD 179143/4) closely resembles that of  $\tau$  Ursae Majoris."

We also have spectra obtained on IIA-O plates at OHP with our BS Cass spectrograph ( $4 \text{ nm mm}^{-1}$ ) in the blue photographic region (380–470 nm). A comparison of those plates with MK standards and peculiar stars observed with the same instrument (Ginestet et al. 1992) obviously indicates the presence of the Am star, which appears to dominate the spectrum in that spectral range. That can explain why Abt & Morrell (1995) did not detect the composite nature of this object even though the K line shows a sharp core upon which an underlying broader line indicates the presence of a cooler star.

As far as the classification of the primary is concerned, Ginestet et al. (1997) proposed a classification for  $\sigma$  Leo of F8–G0 III–IV after comparing the spectrum of  $\sigma$  Leo with those represented in an atlas of MK standards (Carquillat et al. 1997). The latter resulted from a study carried out in

the near-infrared at OHP (Carelec and Aurélie spectrographs, spectral range 840–880 nm,  $3.3 \text{ nm mm}^{-1}$  of dispersion) of stars with composite spectra.

### 3. OBSERVATIONS

#### 3.1. Radial Velocities

It befits a new discussion of the orbit of *o* Leo to include fresh radial velocities to supplement those (some of which are now more than 100 years old) used by Plummer (1908) in the hitherto adopted spectroscopic orbit. The principal source of new velocities, used by both the Toulouse and the Cambridge authors, has been the CORAVEL photoelectric spectrometer (Baranne et al. 1979) on the Swiss 1 m telescope at OHP, which has kindly been made available to us by M. Mayor and the Geneva Observatory. An example of a CORAVEL radial velocity trace is shown in Figure 1. Additional observations, mostly predating any CORAVEL ones, have been made by R. F. G. with the original spectrometer (Griffin 1967) in Cambridge, the one on the 200 inch (5 m) Palomar telescope (Griffin & Gunn 1974), the CORAVEL at ESO, and the spectrometer at the 48 inch (1.2 m) reflector of the Dominion Astrophysical Observatory in Canada (DAO; Fletcher et al. 1982). The new data are set out in Table 1, together with the velocities published from Bonn (Zurhellen 1907), Lick (Plummer 1908), and Texas (Parsons 1983). Observations in which the spectra of the two components are too closely blended to be separable have been omitted. Since, after such omission, there is only one velocity from the Cape Observatory (Lunt 1919; Jones 1928), that too has been omitted from consideration. In Table 1 the first three columns give the date, Julian year, and Modified Julian Date (MJD), respectively. They are followed by the columns for primary and secondary radial velocities and their deviations from those expected on the basis of our orbit (see below). The last column contains an abbreviation for the observatory.

In order to combine the published radial velocities with the new ones, and to obtain the best orbital solution from the ensemble, it has been necessary to make zero-point adjustments to the earlier data sets and to apply suitable weightings to each of the sources of velocities. That has been done by trial solutions, the criteria being to make the mean residual for each data source close to zero and to obtain approximate equality of the weighted variances for all sources. The zero points of all but the CORAVEL data sets have been changed by  $-0.7 \text{ km s}^{-1}$  to match the CORAVEL one; that change has already been made to the velocities listed in Table 1. The weights attributed to the various sources are shown in Table 2. A few observations, marked with a colon in Table 1, have been noted by their authors as uncertain and have been attributed half the weight that they would normally have. The “best” set of observations—those obtained for the primary component with CORAVEL—are taken as having full (unit) weight; the standard deviation corresponding to that weight is slightly less than  $0.5 \text{ km s}^{-1}$ .

#### 3.2. Interferometry

All interferometers used to resolve the components of *o* Leo combine afocal light beams from separate apertures to form interference patterns whose amplitude and phase represent the complex visibility function measured at coordi-

nates  $(u, v)$  corresponding to length and orientation of the projected baselines between the apertures. The  $(u, v)$  coordinates are time-dependent because of the rotation of the Earth. The complex visibility function is the Fourier transform of the stellar brightness distribution, i.e., the conjugate variables to  $(u, v)$  are the sky coordinates  $(\theta_{\text{R.A.}}, \theta_{\text{dec}})$ . The structure of the star can therefore be modeled or imaged from the amplitudes and/or phases of the measured visibilities.

For the Mark III observations, only the north-south baselines of 28.0 m and 31.5 m were used, one at a time. The NPOI was configured as described by Benson et al. (1997) to include three simultaneous baselines between 19 and 38 m. The PTI has a fixed north-south baseline of 100 m.

Each incoherent visibility measurement is the result of (typically) 90–130 s of on-source integration of the squared modulus of the visibility amplitude (bias-corrected for Poisson noise statistics), followed by a measurement of the background on nearby blank sky. The NPOI records the visibility on all three baselines simultaneously. This also allows us to form the complex triple product before coherently integrating it in order to obtain its phase (closure phase), which is free from any atmospheric phase noise (see, e.g., Cornwell 1987). The visibilities were thus measured at 500, 550, and 800 nm with the Mark III, from 530 to 850 nm with NPOI (20 channels), and at  $2.2 \mu\text{m}$  with PTI.

The dates of observation, and the number of visibilities recorded (as well as other results described below) are listed in Tables 3, 4, and 5 for the Mark III, NPOI, and PTI, respectively. Columns (1) and (2) give the date and fractional Julian year of the observations, and column (3) gives the number of measured visibilities. (Cols. [4]–[8] are described in § 4.2.) The Besselian year,  $B_y$ , used in previous publications can be computed from the Julian year,  $J_y$ , as  $B_y = 1.00002136J_y - 0.0414$ .

Procedures for the reduction and calibration of the visibility data were identical to those described by Hummel et al. (1995) (for the Mark III), Hummel et al. (1998) (for NPOI), and Boden et al. (1999a) (for PTI). The calibration of the visibility amplitudes (and closure phases for NPOI) is based on observations of (nearly) unresolved stars, which are interleaved with the program stars. The visibility-amplitude reduction due to atmospheric phase noise and instrumental effects, as well as closure-phase errors due to beam-combiner drifts, can be determined from the calibrator data, since the theoretical response of an interferometer to unresolved stars is known to be unity for the amplitudes and zero for the phases. Any deviations can be parameterized and thus removed from the program-star data. Whereas a measure for the seeing was used to parameterize the visibility amplitude reduction for the Mark III data, we simply adopted time dependence as a parameter for the data of the other interferometers. Data from three selected nights for NPOI and Mark III are shown in Figures 2, 3, 4, 5, and 6. All the PTI data are shown in Figure 7 as a function of scan number.

For calibrators, we used HR 3975 ( $\eta$  Leo) in the visual and HR 3826, HR 3640, and HR 3973 in the infrared. The first calibrator,  $\eta$  Leo, is actually an occultation binary, but the companion was found to be about 5 mag fainter than the primary by Evans et al. (1985), and  $\eta$  Leo has always appeared as single star when observed with the Mark III interferometer. All calibrators appeared single to the *Hipparcos* satellite (ESA 1997). The diameters of the calibrator

TABLE 1  
RADIAL VELOCITY RESULT LOG

DATE	JULIAN YEAR	MJD	PRIMARY		SECONDARY		OBSERVATORY
			(km s <sup>-1</sup> )	O - C	(km s <sup>-1</sup> )	O - C	
Mar 23 .....	1898.2251	14371.22	66.0	-3.17	-29.5	-6.97	Lick
Nov 01 .....	1898.8366	14594.55	-30.7	-2.14	83.9	-4.30	Lick
Nov 02 .....	1898.8393	14595.55	-23.3	-1.36	82.9	2.21	Lick
Nov 06 .....	1898.8502	14599.54	58.9	-0.91	-15.5	-3.58	Lick
Nov 07 .....	1898.8528	14600.50	73.7	-0.76	-31.6	-3.08	Lick
	1898.8533	14600.65	72.5	-3.55	-35.1	-4.77	Lick
Nov 09 .....	1898.8585	14602.56	76.8	0.04	-36.2	-5.07	Lick
Nov 10 .....	1898.8612	14603.54	62.6	-0.91	-14.8	1.32	Lick
Nov 13 .....	1898.8694	14606.56	-2.2	0.79	59.3	0.07	Lick
Nov 14 .....	1898.8721	14607.53	-18.4	1.02	80.9	3.06	Lick
Nov 17 .....	1898.8804	14610.55	-12.7	2.41	70.2	-2.76	Lick
Nov 23 .....	1898.8968	14616.56	82.5	2.36	-32.9	2.06	Lick
Nov 30 .....	1898.9157	14623.47	-25.3	3.36	90.6	2.29	Lick
	1898.9159	14623.52	-27.0	1.60	90.9	2.65	Lick
Dec 01 .....	1898.9185	14624.48	-21.5	1.17	83.5	1.97	Lick
Dec 05 .....	1898.9294	14628.48	57.6	-1.15	-5.4	5.32	Lick
Dec 22 .....	1898.9760	14645.50	81.0	0.63	-33.0	2.21	Lick
Dec 28 .....	1898.9923	14651.45	-23.7	0.54	84.9	1.59	Lick
Jan 24 .....	1899.0660	14678.37	9.2	-2.57	44.0	1.50	Lick
Jan 28 .....	1899.0771	14682.40	-22.2	1.23	84.9	2.51	Lick
Jan 30 .....	1899.0824	14684.34	9.3	-1.26	45.6	1.73	Lick
Feb 15 .....	1899.1264	14700.42	49.4	2.01	-2.1	-4.25	Lick
Feb 16 .....	1899.1291	14701.42	66.4	-0.28	-23.1	-3.39	Lick
Apr 04 .....	1899.2572	14748.18	70.4	1.38	-22.6	-0.24	Lick
Apr 11 .....	1899.2766	14755.27	-17.9	1.02	79.5	2.22	Lick
Jan 11 .....	1900.0299	15030.42	-22.9	-0.17	79.8	-1.80	Lick
Feb 28 .....	1900.1612	15078.38	68.9	2.05	-19.4	0.50	Lick
Apr 05 .....	1900.2593	15114.22	-7.3	0.13	64.2	-0.06	Lick
Apr 14 .....	1905.2851	16949.90	80.1	-0.01	-35.3	-0.38	Bonn
Apr 19 .....	1905.2988	16954.90	3.2	-1.08	57.9	6.91	Bonn
Apr 04 .....	1906.2570	17304.88	-27.6	-1.08	83.6	-2.29	Bonn
Apr 06 .....	1906.2625	17306.88	-19.0	0.57	84.9	6.88	Bonn
Apr 07 .....	1906.2652	17307.87	-3.9	-1.07	56.2	-2.84	Bonn
Apr 09 .....	1906.2706	17309.85	43.8	1.35	10.7	2.96	Bonn
Apr 10 .....	1906.2733	17310.82	64.8	2.38	-15.8	-0.92	Bonn
Apr 11 .....	1906.2761	17311.86	76.3	-0.45	-26.9	4.21	Bonn
Apr 12 .....	1906.2789	17312.87	81.4	0.39	-38.9	-2.96	Bonn
Apr 15 .....	1906.2871	17315.85	38.4	-0.83	5.9	-5.49	Bonn
Apr 20 .....	1906.3007	17320.83	-24.9	0.51	85.8	1.17	Bonn
Mar 09 .....	1908.1855	18009.26	82.0	2.64	-31.8	2.28	Lick
Mar 10 .....	1908.1884	18010.33	62.1:	-5.61	-26.1:	-5.22	Lick
Apr 14 .....	1981.2852	44708.93	-8.9	-0.70	...	...	Cambridge
Apr 17 .....	1981.2933	44711.89	55.5:	-1.91	...	...	Cambridge
Apr 20 .....	1981.3016	44714.90	...	...	-33.1	-0.66	Cambridge
Apr 27 .....	1981.3207	44721.89	-26.0	1.28	...	...	Cambridge
May 02 .....	1981.3345	44726.92	68.3	1.40	...	...	Cambridge
May 19 .....	1981.3789	44743.13	82.3	1.25	...	...	Palomar
May 24 .....	1981.3946	44748.88	-17.3:	0.45	...	...	Cambridge
May 25 .....	1981.3953	44749.13	-19.7	1.35	...	...	Texas
Oct 27 .....	1981.8207	44904.51	61.8	-1.36	-15.5	0.22	Palomar
Jan 11 .....	1982.0275	44980.06	-3.5	0.68	61.2	0.62	Cambridge
Mar 05 .....	1982.1731	45033.24	79.8	-1.11	...	...	Texas
Mar 12 .....	1982.1942	45040.94	-22.6	4.14	89.3	3.16	Cambridge
Apr 14 .....	1982.2844	45073.88	49.5	1.67	0.9	-0.75	Cambridge
May 11 .....	1982.3583	45100.86	1.0	-0.42	54.3	0.07	Cambridge
Nov 25 .....	1982.8995	45298.54	6.0	0.15	49.4	0.19	Palomar
Feb 03 .....	1983.0909	45368.45	62.5	-0.62	-16.0	-0.32	DAO
Jan 09 .....	1984.0208	45708.09	-25.0	-0.04	85.1:	0.98	Cambridge
Jan 03 .....	1986.0067	46433.44	-20.5	-0.32	78.9	0.20	Palomar
Jan 04 .....	1986.0094	46434.44	-4.0	-0.44	59.8	-0.08	Palomar
Mar 05 .....	1986.1751	46494.97	52.9	-0.87	-3.8	1.28	Cambridge
Mar 07 .....	1986.1780	46496.00	72.1	0.56	-25.4	-0.19	Cambridge
Apr 04 .....	1986.2569	46524.85	69.1	-0.40	-21.6	1.30	OHP

TABLE 1—Continued

DATE	JULIAN YEAR	MJD	PRIMARY		SECONDARY		OBSERVATORY
			(km s <sup>-1</sup> )	O - C	(km s <sup>-1</sup> )	O - C	
Nov 26 .....	1986.9021	46760.51	58.8	0.20	-9.6	0.95	Palomar
Feb 21 .....	1987.1389	46847.00	66.6	-0.73	-22.0	-1.56	Cambridge
Feb 28 .....	1987.1607	46854.94	-2.5	-0.07	59.2	0.60	OHP
Mar 01 .....	1987.1634	46855.92	19.3	-0.10	35.7	1.84	OHP
Oct 18 .....	1987.7939	47086.22	-14.8	0.14	71.1	-1.67	OHP
Nov 08 .....	1987.8518	47107.38	74.9	-0.22	-29.6	-0.33	OHP
Jan 26 .....	1988.0681	47186.38	-28.2	-0.12	86.6	-1.06	DAO
Jan 31 .....	1988.0818	47191.39	62.5	-1.05	-16.1	0.06	DAO
Feb 01 .....	1988.0845	47192.37	77.0	0.22	-29.2	1.95	DAO
Mar 10 .....	1988.1902	47230.97	-18.1	0.26	76.6	-0.04	OHP
Apr 30 .....	1988.3296	47281.88	68.2	-0.09	-21.6	-0.07	OHP
May 01 .....	1988.3322	47282.83	51.6	0.91	-1.4	0.19	OHP
May 05 .....	1988.3432	47286.85	-26.4	-0.03	86.3	0.58	OHP
May 06 .....	1988.3460	47287.87	-29.2	-1.13	87.7	0.06	OHP
Oct 25 .....	1988.8150	47459.17	-2.2	0.81	59.1	-0.16	OHP
Oct 27 .....	1988.8205	47461.20	-28.1	0.13	88.3	0.48	OHP
Oct 28 .....	1988.8233	47462.21	-26.5	-0.39	85.8	0.38	OHP
Oct 29 .....	1988.8259	47463.17	-15.6	-0.67	71.2	-1.56	OHP
Oct 30 .....	1988.8287	47464.20	3.9	-0.88	50.3	-0.12	OHP
Oct 31 .....	1988.8315	47465.21	27.9	-0.31	24.2	0.32	OHP
Nov 07 .....	1988.8507	47472.23	29.9	0.31	22.2	-0.12	OHP
Jan 18 .....	1989.0474	47544.07	45.9	1.21	3.0	-2.21	Cambridge
Mar 14 .....	1989.2003	47599.91	78.6	-0.09	-33.2	0.12	OHP
Mar 15 .....	1989.2031	47600.93	67.0	0.16	-18.6	1.29	OHP
Mar 19 .....	1989.2115	47604.00	-0.2	-0.28	55.2	-0.55	OHP
	1989.2140	47604.93	-17.3	-0.54	73.6	-1.23	OHP
Mar 21 .....	1989.2192	47606.83	-27.9	0.16	89.1	1.47	OHP
Mar 22 .....	1989.2223	47607.96	-17.7	0.09	75.1	-0.90	OHP
Mar 23 .....	1989.2250	47608.94	-1.4	-1.04	57.6	1.35	OHP
Mar 30 .....	1989.2441	47615.92	58.5	0.37	-9.3	0.72	OHP
May 02 .....	1989.3343	47648.86	-22.5	-0.09	81.1	-0.13	OHP
Dec 07 .....	1989.9321	47867.20	-28.8	-0.42	88.2	0.21	OHP
Dec 08 .....	1989.9348	47868.20	-25.8	-0.02	85.9	0.85	OHP
Dec 12 .....	1989.9456	47872.13	50.2	-0.30	-0.5	0.88	OHP
Dec 14 .....	1989.9511	47874.14	79.3	-0.17	-34.4	-0.20	OHP
Feb 12 .....	1990.1155	47934.20	69.1	-0.57	-23.3	-0.21	OHP
Mar 13 .....	1990.1970	47963.95	57.0	0.37	-7.7	0.62	OHP
Mar 15 .....	1990.2025	47965.97	10.5	-0.14	43.0	-0.78	OHP
Mar 16 .....	1990.2052	47966.95	-9.4	0.26	64.9	-1.89	OHP
Jan 05 .....	1991.0106	48261.13	-6.0	-1.13	61.6	0.24	OHP
Jan 08 .....	1991.0189	48264.16	61.0	-1.01	-12.8	1.62	OHP
Jan 10 .....	1991.0243	48266.11	81.2	0.16	-36.0	-0.02	OHP
Feb 04 .....	1991.0926	48291.06	15.4	-0.05	39.4	1.07	OHP
Feb 05 .....	1991.0953	48292.07	38.7	-0.57	11.4	0.06	OHP
Dec 19 .....	1991.9634	48609.13	-3.5	0.45	59.2	-1.12	OHP
Feb 19 .....	1992.1329	48671.04	75.7	0.22	-29.2	0.48	OHP
Feb 20 .....	1992.1356	48672.04	81.1	0.06	-35.5	0.47	OHP
Feb 21 .....	1992.1385	48673.08	76.0	-0.06	-30.2	0.13	OHP
Feb 22 .....	1992.1412	48674.06	61.7	-0.50	-14.9	-0.27	OHP
Feb 23 .....	1992.1438	48675.04	42.4	0.45	7.6	-0.71	OHP
Apr 27 .....	1992.3214	48739.90	1.3	-0.68	54.0	0.40	OHP
Dec 11 .....	1992.9436	48967.14	-5.9	0.48	61.6	-1.47	OHP
Dec 12 .....	1992.9464	48968.16	-21.5	0.65	81.7	0.77	OHP
Dec 18 .....	1992.9627	48974.11	52.9	-0.28	-3.9	0.51	OHP
Jan 13 .....	1993.0339	49000.15	-12.3	-0.42	68.5	-0.81	OHP
Feb 19 .....	1993.1348	49037.00	52.9	0.20	-4.0	-0.13	OHP
Nov 05 .....	1993.8450	49296.39	76.9	-0.16	-31.8	-0.33	OHP
Dec 27 .....	1993.9866	49348.11	-10.4	1.37	70.1	0.92	OHP
Jan 10 .....	1994.0247	49362.02	-19.9	0.64	80.1	0.99	OHP
May 04 .....	1994.3392	49476.89	-27.9	0.66	89.5	1.30	OHP
Dec 14 .....	1994.9505	49700.16	73.3	0.61	-26.1	0.41	OHP
Jan 02 .....	1995.0024	49719.13	36.7	0.05	12.5	-1.82	OHP
Apr 02 .....	1996.2530	50175.89	16.3	-1.07	35.1	-1.06	OHP
Jan 25 .....	1997.0666	50473.09	35.2	-0.03	14.7	-1.23	OHP
Dec 22 .....	1997.9730	50804.14	77.9	0.42	-31.0	0.94	OHP

TABLE 2  
WEIGHTINGS FOR THE DIFFERENT SOURCES OF  
RADIAL VELOCITIES

Source	Primary	Secondary
Bonn .....	1/4	1/60
Cambridge.....	1/4	1/6
OHP .....	1	1/3
DAO .....	1/2	1/6
Lick .....	1/15	1/45
Palomar .....	1/2	1/2
Texas.....	1/10	...

stars, small but nevertheless significant, were estimated from a calibration obtained by Mozurkewich et al. (1991) based on the apparent visual magnitude  $V$  and the  $(R-I)$  color index of the stars. The calibrator-star data are listed in Table 6.

It has been noted by Hummel et al. (1998) that the calibration errors tend to dominate the fluctuations in the visibility amplitudes, while the calibrated closure phases are less prone to systematic error because they are not affected by atmospheric phase noise. The quality of the calibration is a direct function of the angular separation between

program and calibrator star. For the most conservative estimate of the calibration error, we determined the standard deviation of all calibrator-star amplitudes (after calibration) and added them in quadrature to the statistical uncertainties.

#### 4. MODELING

In order to determine the distance to  $\alpha$  Leo and the masses,  $\mathcal{M}_1$  and  $\mathcal{M}_2$ , of its components, we must combine the results of spectroscopy and interferometry. One method is to combine orbital elements, i.e., the inclination  $i$  and the values for  $\mathcal{M}_{1,2} \sin^3 i$ , which are derived from the eccentricity  $e$  and period  $P$  of the orbit, as well as from the velocity semi-amplitudes  $K_1$  and  $K_2$ . Another method is to combine the data and to reevaluate the common orbital elements while at the same time including the component masses or velocity semi-amplitudes in the model. This technique effectively reduces the number of free parameters, and we have chosen the component masses in order to avoid the combination of nonlinear fit parameters for their determination. Another, perhaps more efficient, choice has been made by Boden et al. (1999b), and related discussions can be found in Pourbaix (1998) and Pourbaix & Eichhorn (1999). Before combining the data sets, one should make sure that they are mutually consistent by fitting the orbital elements to them separately and then comparing the ones in common. The results discussed below are listed in Table 7.

TABLE 3  
MARK III OBSERVATION AND RESULT LOG

UT Date (1)	Julian Year (2)	Number of Visibilities (3)	$\rho$ (mas) (4)	$\theta$ (deg) (5)	$\sigma_{\text{maj}}$ (mas) (6)	$\sigma_{\text{min}}$ (mas) (7)	$\varphi$ (deg) (8)	$O-C$ (mas) (9)
Dec 08 .....	1990.9345	48	2.66	89.95	0.122	0.050	94.7	0.255
Dec 09 .....	1990.9373	66	2.77	136.55	0.064	0.015	95.2	0.013
Jan 19 .....	1991.0495	55	3.58	44.22	0.065	0.020	87.9	0.143
Feb 04 .....	1992.0926	36	4.15	170.34	0.550	0.088	89.0	0.234
Mar 13 .....	1992.1967	24	4.48	19.09	0.305	0.053	85.2	0.107
Mar 15 .....	1992.2021	36	2.69	52.83	0.281	0.053	87.5	0.362

TABLE 4  
NPOI OBSERVATION AND RESULT LOG

UT Date (1)	Julian Year (2)	Number of Visibilities (3)	$\rho$ (mas) (4)	$\theta$ (deg) (5)	$\sigma_{\text{maj}}$ (mas) (6)	$\sigma_{\text{min}}$ (mas) (7)	$\varphi$ (deg) (8)	$O-C$ (mas) (9)
Feb 04 .....	1997.0947	979	4.22	177.36	0.075	0.030	178.3	0.033
Feb 07 .....	1997.1029	445	3.35	224.23	0.150	0.030	171.9	0.076
Feb 08 .....	1997.1056	623	2.61	255.60	0.095	0.020	178.7	0.077
Feb 15 .....	1997.1248	552	2.79	66.25	0.100	0.030	176.0	0.049
Feb 20 .....	1997.1385	552	4.23	198.34	0.195	0.060	174.5	0.162
Feb 22 .....	1997.1440	276	3.03	235.80	0.255	0.065	176.0	0.109
Feb 26 .....	1997.1549	552	4.18	0.52	0.215	0.060	175.4	0.132
Mar 11 .....	1997.1905	276	2.99	331.78	0.275	0.055	177.4	0.235
Mar 13 .....	1997.1960	644	4.45	7.37	0.180	0.040	173.8	0.065
Mar 14 .....	1997.1987	267	4.26	21.61	0.155	0.065	171.2	0.045
Mar 15 .....	1997.2015	445	3.70	38.36	0.230	0.060	172.2	0.086
Mar 18 .....	1997.2097	450	3.05	149.45	0.205	0.050	175.5	0.168
Mar 21 .....	1997.2179	435	4.23	198.24	0.165	0.055	173.4	0.161
Mar 26 .....	1997.2316	828	3.67	344.09	0.135	0.045	174.3	0.034
Apr 15 .....	1997.2863	457	2.37	105.18	0.120	0.040	171.5	0.104
Apr 18 .....	1997.2945	340	4.33	185.99	0.210	0.070	166.8	0.129
Apr 19 .....	1997.2973	492	4.43	198.18	0.080	0.030	171.4	0.046
May 07 .....	1997.3466	246	2.43	298.00	0.165	0.045	167.7	0.102

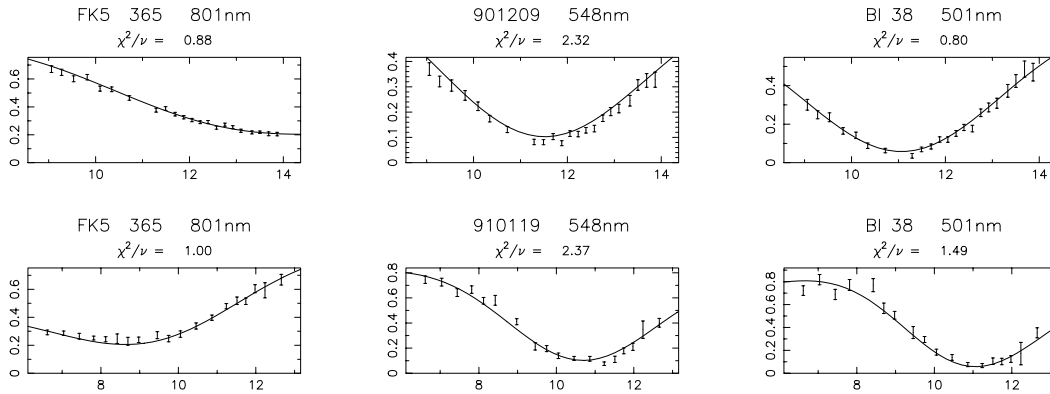


FIG. 2.—Mark III squared visibility amplitudes vs. UT in hours for two selected nights (*date in yymmdd format above middle panel*). The baseline ID (38) is for the north-south baseline of 31.5 m length. Solid line is combined model with 500 nm magnitude difference determined from Mark III data alone.

4.1. Spectroscopic Orbit

The radial velocity data and residuals are shown in Figures 8 and 9 for the primary and secondary, respectively. The fourth column of Table 7 lists the elements for the spectroscopic orbit; that orbit is consistent with being circular and we consequently adopted zero for the eccentricity, but we quote the uncertainty estimate as if the eccentricity were a free parameter. The uncertainty estimates are square-root results of the diagonal elements of the covariance matrix (i.e., formal errors); the resulting goodness-of-fit parameter, the reduced  $\chi^2$ , is also given in the table.

4.2. Visual Orbit

For the second column of Table 7 we fitted a visual orbit to separations and position angles determined with each night's data from NPOI and the Mark III. The PTI data do not sufficiently constrain this type of fit. The astrometric data and orbit are shown in Figure 10 and are listed in Tables 3 and 4, where columns (4) and (5) give the derived separation and position angle (equinox is the mean epoch at local midnight on the date of the observation), columns (6)–(8) the semiaxes and the position angle of the astrometric uncertainty ellipse, and column (9) the deviation of the

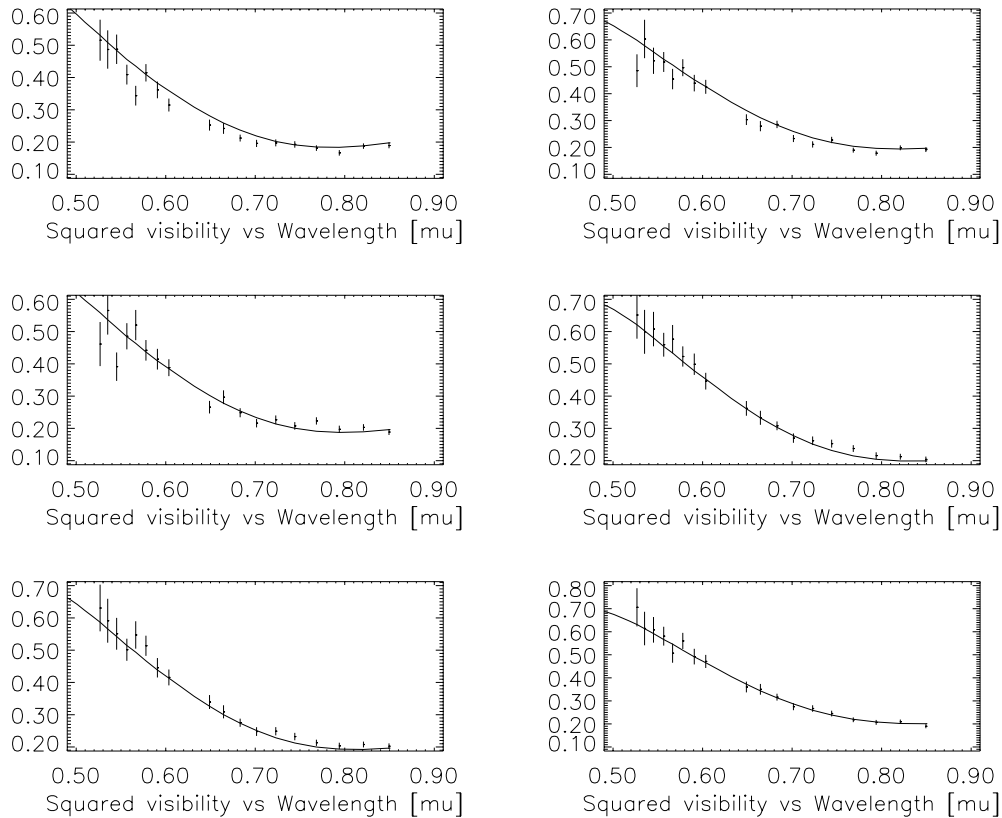


FIG. 3.—NPOI data on the east-west baseline for six scans obtained about every 10 minutes between 6:17 UT and 7:15 UT on 1997 February 8 (*top to bottom, left to right*). For every scan, the visibilities are plotted versus wavelength for the 20 reddest channels of the spectrometer used in the analysis. Line is the combined model.

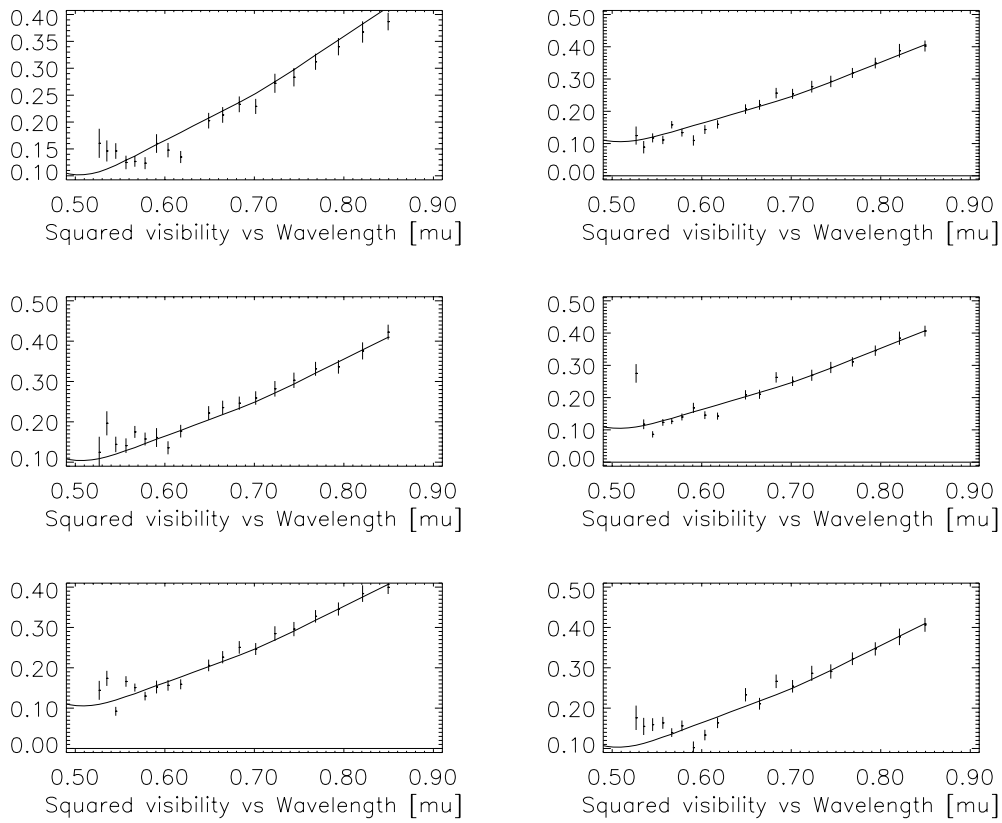


FIG. 4.—NPOI data on the center-west baseline; same scans as in Fig. 3

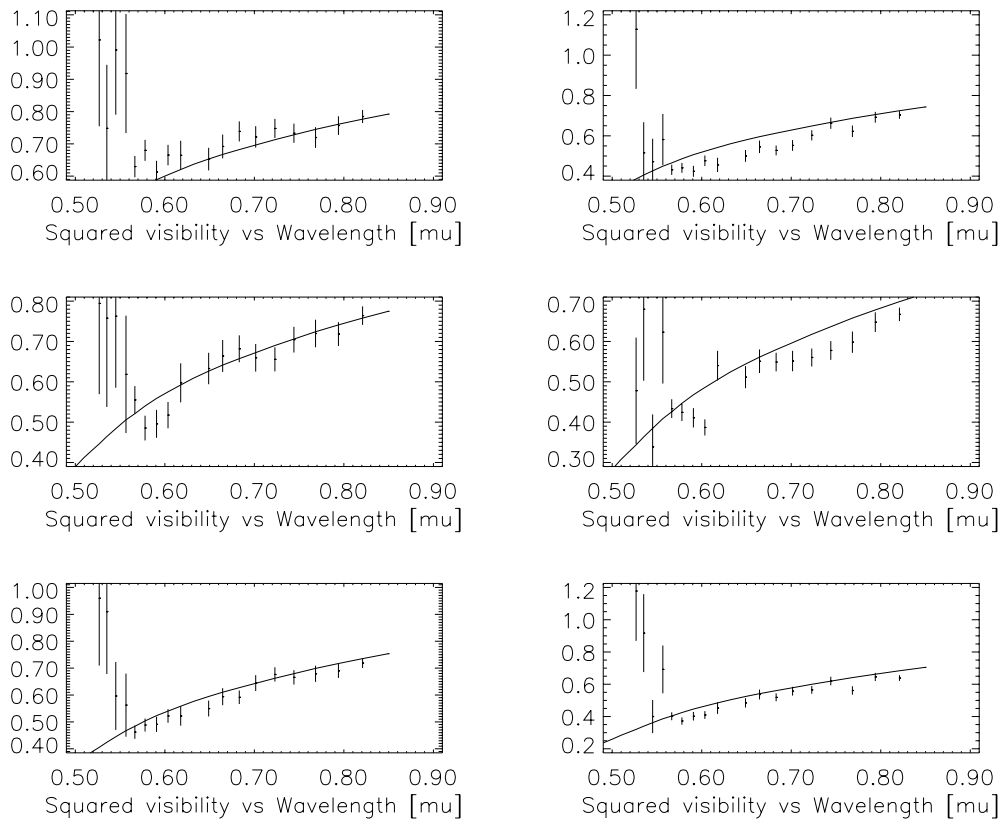


FIG. 5.—NPOI data on the center-east baseline; same scans as in Fig. 3

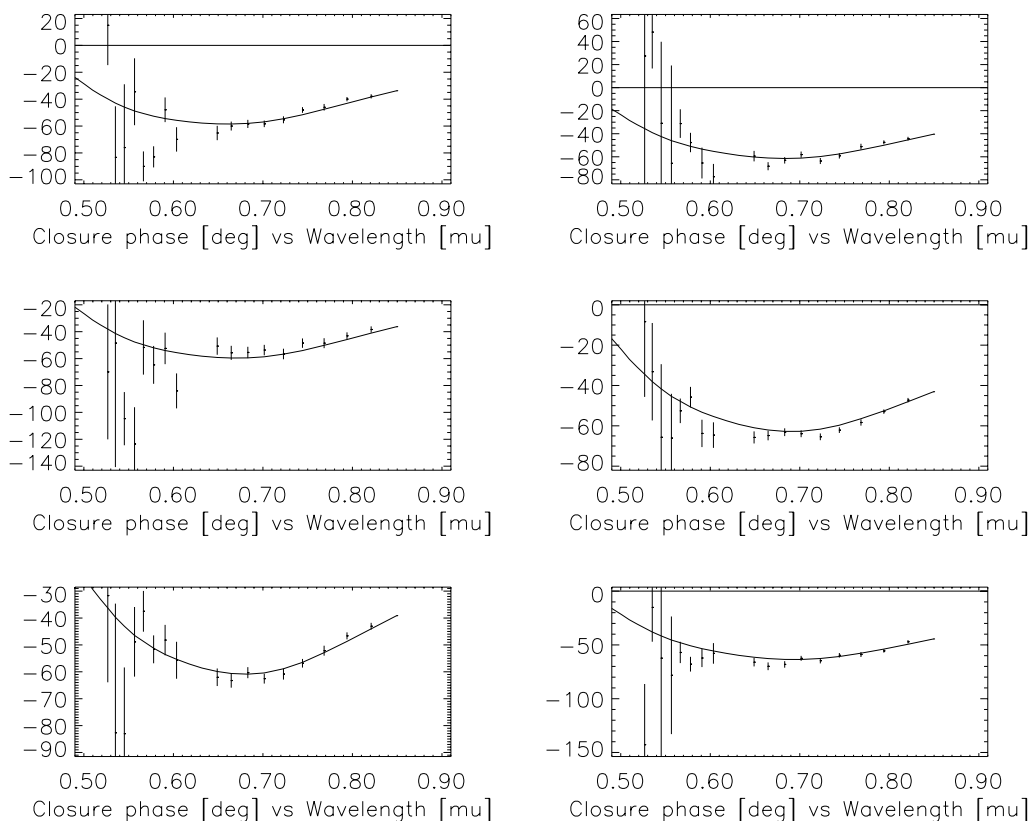


FIG. 6.—NPOI closure-phase data; same scans as in Fig. 3

fitted relative binary position ( $\rho, \theta$ ) from the combined model prediction (see below). Position angles are measured counterclockwise from north. Because of the comparatively short orbital period, we have taken orbital motion during a night (predicted from the combined model; see below) into account. The astrometric uncertainty ellipses correspond in

shape to a Gaussian fitted to the center of the synthesized point-spread function and are scaled in size to match the observed rms of the  $O - C$  values.

For the third column of Table 7 we discarded the intermediate astrometric data (though they are useful when plotting the visual orbit) in favor of the visibility data themselves. This approach provides for a more direct and robust fit, as shown by Hummel et al. (1995) and as reflected in the smaller (formal) uncertainty estimates for the parameters. That effect is mostly a result of the fact that the intermediate astrometric data (i.e., the relative positions) are not

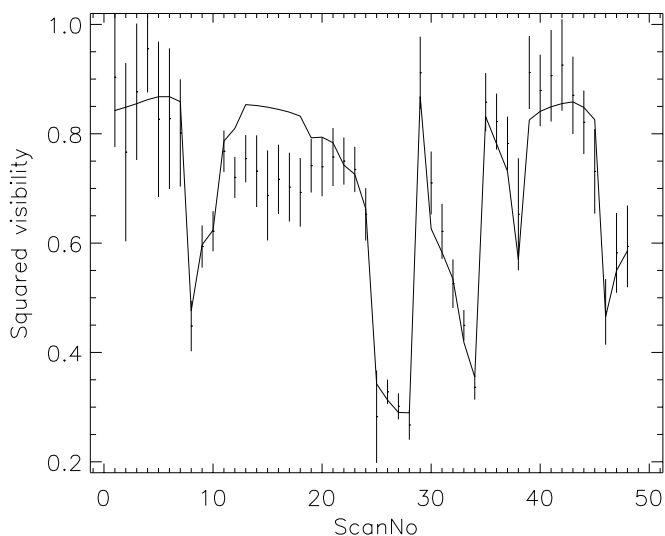


FIG. 7.—PTI squared visibility amplitudes vs. scan number. Refer to Table 5 for the association between dates and scan numbers. The line is a model fit as described in the text.

TABLE 5  
PTI OBSERVATION LOG

UT Date	Julian Year	Number of Visibilities	$\rho$ (mas)	$\theta$ (deg)
Mar 01 .....	1999.1615	6	4.46	191.47
Mar 09 .....	1999.1834	1	4.29	21.77
Mar 19 .....	1999.2107	5	2.41	274.33
Mar 31 .....	1999.2435	7	4.20	204.72
Apr 15 .....	1999.2845	5	3.90	212.23
Apr 16 .....	1999.2873	4	3.04	234.67
Nov 24 .....	1999.8962	1	4.46	12.90
Nov 26 .....	1999.9015	5	3.36	45.27
Nov 28 .....	1999.9071	3	2.51	122.41
Nov 30 .....	1999.9123	1	4.04	173.88
Dec 01 .....	1999.9150	2	4.44	187.92
Dec 02 .....	1999.9179	5	4.28	202.30
Dec 07 .....	1999.9316	3	3.88	350.13

TABLE 6  
CALIBRATION-STAR DATA

Star	Name	Spectral Type	V Magnitude	Sky Separation (deg)	Adopted Angular Diameter (mas)
HR 3975.....	$\eta$ Leo	A0 Ib	3.52	10	$0.67 \pm 0.07$
HR 3826.....	8 Leo	K1 III	5.69	7	$1.09 \pm 0.20$
HR 3640.....	79 Cnc	G5 III	6.01	14	$0.93 \pm 0.10$
HR 3973.....	14 Sex	K1 III	6.21	8	$0.84 \pm 0.06$

well constrained, because the angular scale of the binary is small compared with the fringe spacing for NPOI (and the Mark III), which is about 3 mas. In this case, calibration errors have a bigger effect on the intermediate data, and the fit of these data is of a lower quality. For that reason, the astrometric uncertainty ellipses are larger by about a factor of 5 than the sizes corresponding to an increase of  $\chi^2$  by one for the fits to each night's data.

#### 4.3. Combined Modeling

The individual fit results indicate that they are consistent with a circular orbit, which we adopt in the following. The periastron angle  $\omega$  is taken to be zero, which leaves only a few orbital elements in common between the visual and spectroscopic orbits. Since we quote formal uncertainties for the parameters of the individual fits but suspect that the actual uncertainty estimates are likely to be larger, on the basis of an empirical analysis of how much parameter values changed as new data were added or recalibrated (especially for the NPOI and Mark III data) during the phase of computing solutions for  $\alpha$  Leo, we do not consider the differences for the common elements significant. Therefore we now combine the radial velocity data and the visibility data. We chose to assign the same weight to the interferometric and spectroscopic data in the combined fit,

i.e., we did not rescale the measurement uncertainties for velocities and visibilities. Individually and combined the fits yield values near unity for the reduced  $\chi^2$ . We determined the final values for the orbital elements (including the systemic velocity  $\gamma$ ), masses, and also the magnitude differences between the components. The stellar diameters are too small to be determined reliably and were estimated as described in § 5. Those results are given in the first column of Table 7. Note that  $T$  is the epoch for the binary passing through the ascending node  $\Omega$ .

The magnitude difference at 500 nm is very poorly constrained by the NPOI data alone (shortest wavelength 530 nm). We therefore determined that parameter from a separate fit to the Mark III data using the orbital elements from the combined model. We assigned a larger uncertainty to the magnitude difference at 500 nm because of its deviation from the NPOI result. The magnitude differences obtained from the fit for the other two Mark III channels were, however, consistent within their uncertainties with the results from NPOI as given in Table 7. We interpolated magnitude differences for other NPOI channels using polynomials supported at the wavelengths for which we quote values in the table. The magnitude difference at 2.2  $\mu\text{m}$  was determined from the PTI data using the elements of the combined fit, as well as the adopted component diameters.

TABLE 7  
ORBITAL ELEMENTS AND COMPONENT PARAMETERS

Parameter	Combined Solution	Astrometry	Interferometry	Spectroscopy
$a$ (mas) .....	$4.46 \pm 0.01$	$4.47 \pm 0.04$	$4.47 \pm 0.01$	...
$i$ (deg).....	$57.6 \pm 0.1$	$57.2 \pm 0.7$	$57.4 \pm 0.1$	...
$\Omega$ (deg) (J2000.0).....	$191.4 \pm 0.1$	$191.6 \pm 0.7$	$191.0 \pm 0.1$	...
$T$ (JD - 244E4) .....	$10629.831 \pm 0.003$	$10629.80 \pm 0.04$	$10629.80 \pm 0.01$	$6077.445 \pm 0.003$
$e$ .....	0	$0.0 \pm 0.003$	$0.0026 \pm 0.0010$	$0.0 \pm 0.002$
$P$ (days) .....	$14.498064 \pm 0.000009$	$14.4980 \pm 0.0007$	$14.49789 \pm 0.00004$	$14.498080 \pm 0.000009$
$\mathcal{M}_1 (M_\odot)$ .....	$2.12 \pm 0.01$	...	...	...
$\mathcal{M}_2 (M_\odot)$ .....	$1.87 \pm 0.01$	...	...	...
$\phi_1$ (mas).....	$1.2^a$	...	...	...
$\phi_2$ (mas).....	$0.5^a$	...	...	...
$\Delta m_{500 \text{ nm}}$ (mag) <sup>b</sup> .....	$0.70 \pm 0.10$	...	$0.85 \pm 0.01$	...
$\Delta m_{550 \text{ nm}}$ (mag) .....	$0.91 \pm 0.05$	...	$0.89 \pm 0.01$	...
$\Delta m_{700 \text{ nm}}$ (mag) .....	$1.05 \pm 0.05$	...	$1.05 \pm 0.05$	...
$\Delta m_{850 \text{ nm}}$ (mag) .....	$1.16 \pm 0.05$	...	$1.16 \pm 0.05$	...
$\Delta m_{2200 \text{ nm}}$ (mag) .....	$1.49 \pm 0.05$	...	$1.52 \pm 0.04$	...
$\gamma$ (km s <sup>-1</sup> ).....	$26.18 \pm 0.05$	...	...	$26.18 \pm 0.05$
$K_1$ (km s <sup>-1</sup> ) .....	$54.84^c$	...	...	$54.80 \pm 0.08$
$K_2$ (km s <sup>-1</sup> ) .....	$62.12^c$	...	...	$62.08 \pm 0.16$
$\chi_{\text{red}}^2$ .....	1.18	...	1.17	1.01

<sup>a</sup> Adopted from photometry (see Table 8).

<sup>b</sup>  $\Delta m \equiv m_2 - m_1$ .

<sup>c</sup> Derived for comparison.

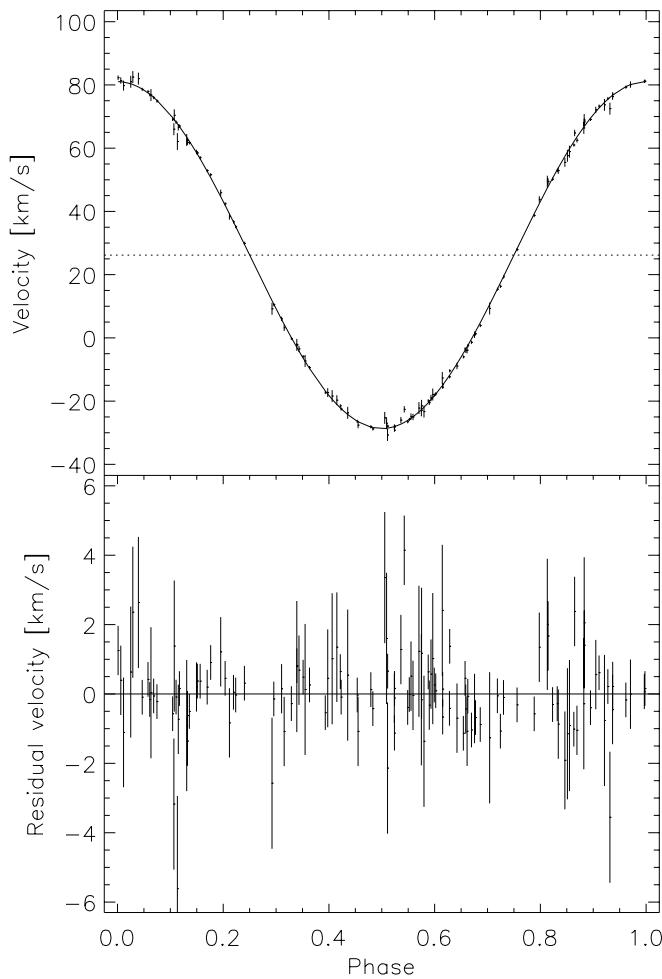


FIG. 8.—Spectroscopic orbit of the primary and residuals from the combined model.

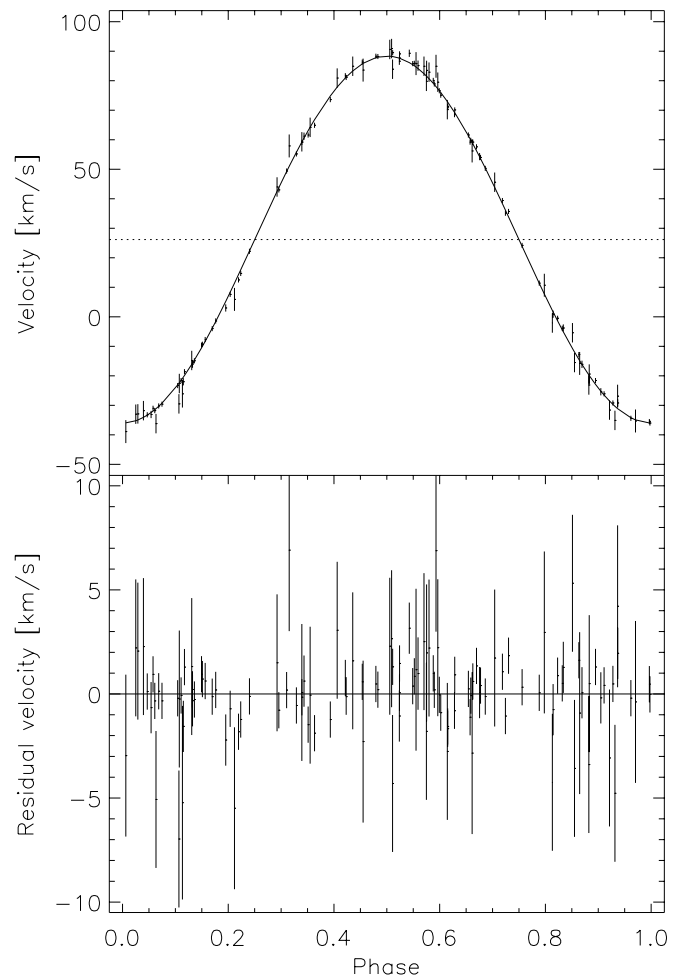


FIG. 9.—Same as Fig. 8, but for the secondary

The resulting fit to the 28 scans from PTI is shown in Figure 7.

5. DISCUSSION

The derived physical parameters of *o* Leo are listed in Table 8. From the orbital period, semimajor axis, and component masses we compute an orbital parallax of  $\pi_{orb} = 24.2 \pm 0.1$  mas, which compares very well to the trigonometric parallax determined by *Hipparcos* (ESA 1997),

TABLE 8  
DERIVED PHYSICAL PARAMETERS OF *o* LEONIS

Parameter	Primary (F9 III)	Secondary (A5m)
$D$ (pc) .....	$41.4 \pm 0.1$	$41.4 \pm 0.1$
$m_V - M_V$ .....	$3.09 \pm 0.01$	$3.09 \pm 0.01$
$B - V$ .....	$0.61 \pm 0.06$	$0.25 \pm 0.08$
$R - I$ .....	$0.26 \pm 0.05$	$0.14 \pm 0.07$
$M_V$ .....	$0.82 \pm 0.03$	$1.73 \pm 0.05$
$M_K$ .....	$-0.41 \pm 0.03$	$1.08 \pm 0.05$
$T_{eff}$ (K) .....	$6000 \pm 200$	$7600 \pm 400$
$BC$ .....	$-0.09 \pm 0.06$	$0.02 \pm 0.05$
$M_{bol}$ .....	$0.73 \pm 0.07$	$1.75 \pm 0.07$
$L$ ( $L_\odot$ ) .....	$39.4 \pm 2.4$	$15.4 \pm 1.0$
$R$ ( $R_\odot$ ) .....	$5.9 \pm 0.5$	$2.2 \pm 0.3$
$D$ (mas) .....	$1.31 \pm 0.23$	$0.49 \pm 0.14$
$\phi_{UD}$ (mas) .....	$1.13 \pm 0.06$	$0.54 \pm 0.03$

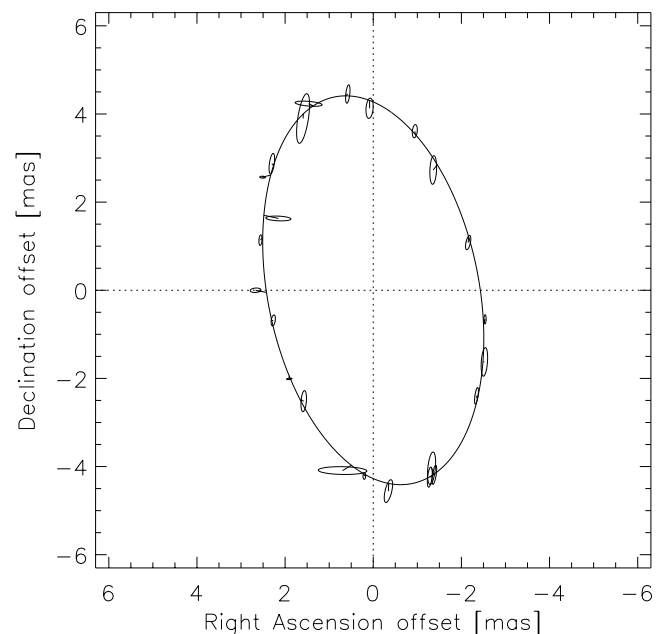


FIG. 10.—Apparent interferometric orbit of *o* Leo, with the combined model. Data are for Mark III and NPOI only.

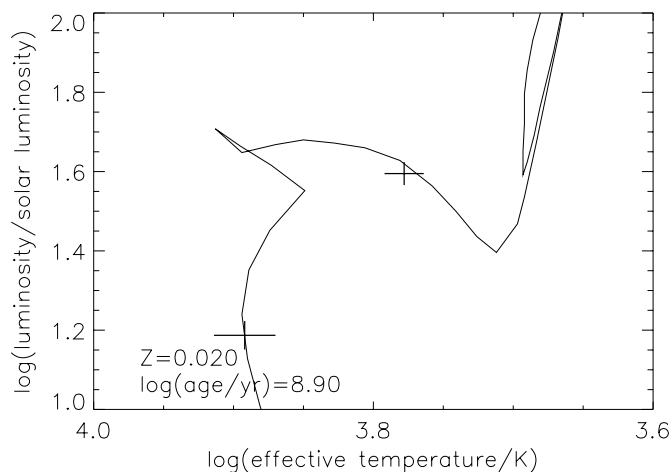


FIG. 11.—Evolutionary status of the  $\alpha$  Leonis stars at age  $10^{8.9}$  yr. The curve is an isochrone from Bertelli et al. (1994).

$\pi_{\text{trig}} = 24.12 \pm 0.97$  mas. Because of the small distance to the star, we will ignore interstellar extinction in the following. From the parallax we compute the distance modulus and use it to obtain absolute combined magnitudes from the apparent magnitudes given by Johnson et al. (1966) for the bands of  $B$  (4.01),  $V$  (3.52),  $R$  (3.11),  $I$  (2.88), and  $K$  (2.43). We extrapolate the magnitude difference in  $B$  from the value at 500 nm by means of a low-order polynomial fit to the measured magnitude differences, and obtain  $\Delta m_{440 \text{ nm}} = 0.55 \pm 0.10$  mag. Equating the fit wavelengths of 440, 550, 700, and 850 nm with the Johnson bands of  $B$ ,  $V$ ,  $R$ , and  $I$ , respectively, we derive individual component magnitudes and  $(B-V)$  and  $(R-I)$  colors. Obviously our filters do not correspond exactly to the Johnson filters, but, given our measurement precision, we can neglect the differences.

The derived  $(B-V)$  colors are consistent with stars of type F9 (0.60) and A5 (0.15), according to tables given in Flower (1977) and Schmidt-Kaler (1982). We adopted values for the effective temperatures (given in Table 8) between the estimates based on the spectral types and those based on a relation between effective temperatures and the  $(B-V)$  color index given by Flower (1996). The uncertainty estimates for the effective temperatures include both extremes.

The bolometric correction  $BC$  can now be determined from the effective temperature estimates and the cali-

brations published by Gubochkin & Miroschnichenko (1991) and Flower (1996). Those two agree well enough (to within 0.05 mag) for us to derive the bolometric magnitudes and luminosities. Table 8 also contains estimates, based on the temperatures and luminosities, for the component radii  $R$  and the corresponding angular diameters  $D$ . The latter can be compared to the (uniform-disk) angular diameters  $\phi$  derived from the  $(R-I)$  color indices and the apparent visual magnitudes, through the calibration derived by Mozurkewich et al. (1991). In view of the smallness of the diameters, their differences are negligible for the fit results.

For a comparison of the physical parameters of the  $\alpha$  Leonis stars with stellar evolution models, we use the isochrones published by Bertelli et al. (1994) for metallicities of  $Z = 0.0004, 0.004, 0.008, 0.02,$  and  $0.05$ . We find a good match with the  $Z = 0.02$  isochrone for an age of  $10^{8.9}$  yr. That fit is shown in Figure 11. The component parameters (including photometry based on the calibrations used by Bertelli et al. 1994 for comparison) predicted by the selected stellar model are listed in Table 9. In that table, we also quote (for the main-sequence component only) the luminosity predicted by a polynomial fit to the mass-luminosity relationship as published by Andersen (1991). The quality of the fit is satisfactory.

## 6. CONCLUSIONS

We have shown how precise stellar masses can be determined from a combination of high-quality radial velocities with the high-resolution capabilities of long-baseline interferometers. A database still dominated by the results of eclipsing-binary studies is being added to by interferometers, which are able to address a much larger number of systems with any orientation in the sky. Future observations should also add to the body of evidence that combined modeling is beneficial to the precise and reliable determination of binary parameters. One area of improvement necessary to achieve stricter constraints on the stellar evolution models remains the photometric calibration of the interferometric data.

We thank the observers D. Black, B. Burrell, C. S. Denison, and L. Rarogiewicz for their careful operation of the Mark III and NPOI arrays, as well as NPOI team members for their support of this project. The work done with the NPOI interferometer was performed through a collaboration between the Naval Research Lab and the US Naval Observatory in association with Lowell Observatory, and was funded by the Office of Naval Research and the Oceanographer of the Navy. Part of the work described here was also performed at the Jet Propulsion Laboratory (JPL), California Institute of Technology, under contract with NASA. Interferometer data were obtained at the Palomar Observatory with the NASA Palomar Testbed Interferometer, which is supported by NASA contracts to the JPL. We thank also S. Udry for the reduction of the CORAVEL observations, and E. Griffin for useful comments. This research has made use of the SIMBAD literature database, operated at CDS, Strasbourg, France.

TABLE 9

COMPONENT PARAMETERS PREDICTED BY THE MODEL ISOCHRONE

Parameter	Primary	Secondary
$M (M_{\odot})$ .....	2.21	1.85
$B-V$ .....	0.61	0.21
$M_V$ .....	0.74	1.71
$T_{\text{eff}} \text{ (K)}$ .....	5950	7800
$M_{\text{bol}}$ .....	0.70	1.76
$L (L_{\odot})$ .....	...	14.0

## REFERENCES

- Abt, H. A., & Morrell, N. I. 1995, *ApJS*, 99, 135
- Africano, J. L., Evans, D. S., Fekel, F. C., Smith, B. W., & Morgan, C. A. 1978, *AJ*, 83, 1100
- Andersen, J. 1991, *A&A Rev.*, 3, 91
- Anderson, J. A. 1920, *ApJ*, 51, 263
- Armstrong, J. T., et al. 1998, *ApJ*, 496, 550
- Babcock, H. W. 1958, *ApJS*, 3, 141
- Bahng, J. D. R. 1958, *ApJ*, 128, 572
- Baily, F. 1845, *The Catalogue of Stars of the British Association* (London: R. & J. E. Taylor), 180
- Baranne, A., Mayor, M., & Poncet, J. L. 1979, *Vistas Astron.*, 23, 279
- Batten, A. H. 1967, *Publ. Dom. Astrophys. Obs. Victoria*, 13, 119
- Batten, A. H., Fletcher, J. M., & MacCarthy, D. G. 1989, *Publ. Dom. Astrophys. Obs. Victoria*, 17, 1
- Benson, J. A., et al. 1997, *AJ*, 114, 1221
- Bertelli, G., Bressan, A., Chiosi, C., Fagotto, F., & Nasi, E. 1994, *A&AS*, 106, 275
- Bidelman, W. P. 1951, *ApJ*, 113, 304
- Boden, A. F., et al. 1999a, *ApJ*, 515, 356
- . 1999b, *ApJ*, 527, 360
- Campbell, W. W. 1898a, *ApJ*, 8, 123
- . 1898b, *ApJ*, 8, 291
- . 1899, *PASP*, 11, 54
- Cannon, A. J., & Pickering, E. C. 1919, *Ann. Astron. Obs. Harvard Coll.*, 94, 76, 289
- Carquillat, J.-M., Jaschek, C., Jaschek, M., & Ginestet, N. 1997, *A&AS*, 123, 5
- Colavita, M. M., et al. 1999, *ApJ*, 510, 505
- Cornwell, T. J. 1987, *A&A*, 180, 269
- ESA. 1997, *The Hipparcos and Tycho Catalogues* (ESA SP-1200) (Noordwijk: ESA)
- Evans, D. S., Edwards, D. A., Frueh, M., McWilliam, A., & Sandmann, W. H. 1985, *AJ*, 90, 2360
- Fletcher, J. M., Harris, H. C., McClure, R. D., & Scarfe, C. D. 1982, *PASP*, 94, 1017
- Flower, P. J. 1977, *A&A*, 54, 31
- . 1996, *ApJ*, 469, 355
- Frost, E. B., Barrett, S. B., & Struve, O. 1929, *Publ. Yerkes Obs.*, vol. VII, pt. I
- Ginestet, N., Carquillat, J.-M., Jaschek, C., & Jaschek, M. 1997, *A&AS*, 123, 135
- Ginestet, N., Carquillat, J.-M., Jaschek, M., Jaschek, C., Pédoussaut, A., & Rochette, J. 1992, *Atlas de Spectres Stellaires* (Toulouse: Centre Régional de Documentation Pédagogique)
- Griffin, R., & Griffin, R. 1986, *J. Astrophys. Astron.*, 7, 195
- Griffin, R. F. 1967, *ApJ*, 148, 465
- . 1999, *Observatory*, 119, 272
- Griffin, R. F., & Gunn, J. E. 1974, *ApJ*, 191, 545
- Gubochkin, A. N., & Miroshnichenko, A. S. 1991, *Kinematika i Fiz. Nebesnykh Tel.*, 7, 64
- Hoffleit, D., & Jaschek, C. 1982, *The Bright Star Catalogue*, (4th ed.; New Haven: Yale Univ. Obs.)
- Hummel, C. A., Armstrong, J. T., Buscher, D. F., Mozurkewich, D., Quirrenbach, A., & Vivekanand, M. 1995, *AJ*, 110, 376
- Hummel, C. A., Mozurkewich, D., Armstrong, J. T., Hajian, A. R., Elias, N. M., II, & Hutter, D. J. 1998, *AJ*, 116, 2536
- Johnson, H. L., Iriarte, B., Mitchell, R. I., & Wiśniewski, W. Z. 1966, *Comm. Lunar Planet. Lab.*, 4, 99
- Jones, H. S. 1928, *Ann. Cape Obs.*, 10, No. 8
- Lunt, J. 1919, *ApJ*, 50, 161
- Markowitz, A. H. 1969, Ph.D. thesis, Ohio State Univ.
- Maury, A. 1897, *Ann. Astron. Obs. Harvard Coll.*, 28, 93
- Mermilliod, J.-C., & Mermilliod, M. 1994, *Catalogue of Mean UBV Data on Stars* (New York: Springer), 518
- Merrill, P. W. 1922, *ApJ*, 56, 40
- McAlister, H. A., Mason, B. D., Hartkopf, W. I., & Shara, M. M. 1993, *AJ*, 106, 1639
- Mozurkewich, D., et al. 1991, *AJ*, 101, 2207
- Parsons, S. B. 1983, *ApJS*, 53, 553
- Plummer, H. C. K. 1908, *Lick Obs. Bull.*, 5, 21
- Pourbaix, D. 1998, *A&AS*, 131, 377
- Pourbaix, D., & Eichhorn, H. 1999, *A&AS*, 136, 419
- Robertson, J. 1940, *Catalog of 3539 Zodiacal Stars for the Equinox 1950.0* (Washington: US Nautical Almanac Office)
- Schmidtke, P. C. 1979, *PASP*, 91, 674
- Schmidt-Kaler, T. H. 1982, in *Landolt-Börnstein New Series, Group 6, vol. 2b, Stars and Star Clusters*, ed. K. Schaifers & H.-H. Voigt (New York: Springer)
- Shao, M., et al. 1988, *A&A*, 193, 357
- Struve, O., & Morgan, W. W. 1927, *ApJ*, 66, 135
- Zurhellen, W. 1907, *Astron. Nachr.*, 173, 353